

ChemComm

Accepted Manuscript



This is an *Accepted Manuscript*, which has been through the Royal Society of Chemistry peer review process and has been accepted for publication.

Accepted Manuscripts are published online shortly after acceptance, before technical editing, formatting and proof reading. Using this free service, authors can make their results available to the community, in citable form, before we publish the edited article. We will replace this *Accepted Manuscript* with the edited and formatted *Advance Article* as soon as it is available.

You can find more information about *Accepted Manuscripts* in the [Information for Authors](#).

Please note that technical editing may introduce minor changes to the text and/or graphics, which may alter content. The journal's standard [Terms & Conditions](#) and the [Ethical guidelines](#) still apply. In no event shall the Royal Society of Chemistry be held responsible for any errors or omissions in this *Accepted Manuscript* or any consequences arising from the use of any information it contains.

COMMUNICATION

Disodium Diselenide in Colloidal Nanocrystals: Acting as an Anion Exchange Precursor, Metal Selenide Precursor, and Chalcogenide Ligand

Cite this: DOI: 10.1039/x0xx00000x

Received 00th January 2012,
Accepted 00th January 2012Donghyeuk Choi,^a Seungyeol Lee,^a Junho Lee,^b Kyung-Sang Cho,^{*b} Sang-Wook Kim^{*a}

DOI: 10.1039/x0xx00000x

www.rsc.org/

New application areas using very simple alkali metal chalcogenide, disodium diselenide (Na_2Se_2), has been developed. Prepared alkali metal chalcogenides (disodium diselenide, Na_2Se_2) are acting as an anionic exchange precursor (PbS to PbS/PbSe), Se precursor for metal selenide nanoparticles (Ag to Ag_2Se), and MCCs (FeO-MCCs) depending on the type of colloidal nanoparticles.

A metal Chalcogenide consisting of at least one chalcogen anion and counter electropositive cation is one of the most fascinating chemical compound due to fast-ion conductivity of open-framework chalcogenides¹, high photoluminescence of cadmium chalcogenides², infrared transparency of chalcogenide glasses³, and high electron mobility of chalcogenide ligand.⁴ Almost all the chemical elements in group 16 of the periodic table are defined as chalcogens, chalcogenide is more commonly indicated to sulfides, selenides, and tellurides, rather than oxides. Chalcogenide exist in a variety of forms depending on the counter electropositive cation such as alkali metal chalcogenide, transition metal chalcogenides and main group chalcogenides. During the past, Chalcogenide have been intensively researched about transition metal chalcogenides (semiconductor nanocrystal, Q-dot)^{5,6,7,8} and main group chalcogenides (molecular metal chalcogenide, MCCs)^{4,9,10} respectively. Recently, molecular metal chalcogenide, which is one of the main group chalcogenides, have attracted considerable attention because they can replace the passivation ligands of the colloidal nanoparticles, as a result, all inorganic nanoparticle system are realized.¹⁰

Colloidal nanocrystals with a narrow size distribution and uniform shape are important for their application. They are determined by many reaction conditions, especially, surfactants are clincher in the colloidal synthetic system. The surfactant, which have hydrophilic head group and long alkyl chain tail group can prevent aggregation of particles and control the size and shape.^{11,12} Despite its usability in various nanocrystals, it limit the research on the device using colloidal nanocrystal due to their insulating property in solid-state device and chemical instability of hydrocarbon ligand in the device

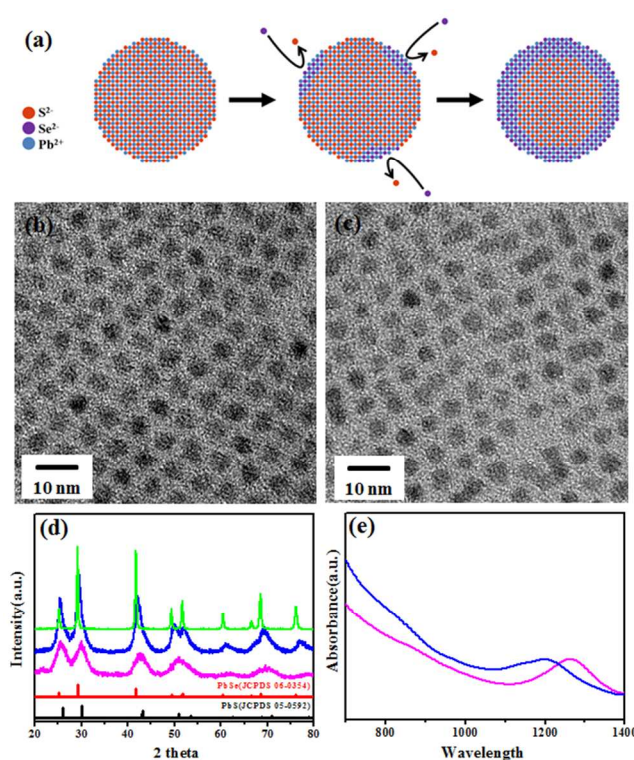


Figure 1. (a) A schematic illustration of anion exchange by Se^{2-} ions in the PbS core. TEM image of (b) bare PbS, (c) PbS- Na_2Se_2 molar ratio 4 : 1. (d) X-ray diffraction patterns of bare PbS (pink), PbS- Na_2Se_2 molar ratio 4 : 1 (blue), PbS- Na_2Se_2 molar ratio 1 : 4 (green) (e) Absorbance of bare PbS (Pink), PbS- Na_2Se_2 molar ratio 4 : 1 (Blue)

manufacturing process.^{9,13} To overcome these challenges, a few groups have reported inorganic ligand to improve its electrical conductivity and chemical stability. For example, Talapin group

synthesized inorganic ligand so called molecular metal chalcogenide complexes (MCCs) which use main group metal and investigated electric conductivity and FET properties of colloidal nanocrystal-MCCs film.^{4,9,10}

Metal chalcogenides with alkali metals also manifest a huge potential as inorganic ligands; however, unlike main group chalcogenides, limited research has been carried out regarding their synthesis and application. In this study, we present an alkali metal chalcogenide, disodium diselenide (Na_2Se_2), which is prepared according to the literature with slight modifications, for use as a new type MCC.¹⁴ We found that Na_2Se_2 molecules could fit into a variety of roles, such as that of an anionic exchanger, a Se precursor for metal selenide nanoparticles, and an anionic surfactant for MCCs depending on the type of nanoparticles such as Q-dot, metal nanoparticles, and metal oxide nanoparticles.

Na_2Se_2 molecules were synthesized by mixing selenium and sodium precursors in anhydrous ethanol. The detailed experimental procedure and analytic data are provided in the supporting information section.

In alloy and core/shell nanocrystals, composition control has received considerable attention due to the resulting variable physical and optical properties. Cationic and anionic exchange method is one of the available methods to change the composition of the nanocrystals, however, it is not easy because the exchange of the component especially, anion of the nanocrystal needs huge activation energy, therefore, high temperatures or pressures in order to diffuse the atom through a nanocrystal.^{15,16} As an alternative, application of new precursor, for example, Na_2Se_2 to the exchange reaction can be considered.

Figure 1a is schematic illustration of anion exchange reaction by the following experimental results, showing that Se^{2-} ion replaces S^{2-} ion near the surface, which the homogeneous PbS nanoparticles transform to PbS/PbSe core/shell nanoparticles. They showed that as prepared PbS and the resulting PbS/PbSe (PbS : Na_2Se_2 = 4 : 1) nanoparticles have the similar sizes of 4.5 nm ($\sigma=0.37$) and 4.1 nm ($\sigma=0.36$), respectively. (Figure 1b and 1c) The similar size of nanoparticles before and after reaction is an evidence of anion exchange reaction between PbS and Na_2Se_2 . Low magnification Transmission electron microscopy (TEM) images in the supporting information show that both have uniform size distribution. (Figure S1) The TEM image of PbS nanoparticle to Se precursor molar ratio of 1 : 4, as shown in figure S2, revealed that as-synthesized PbSe nanoparticles aggregated with each other and larger than original PbS. The high-resolution TEM (HR-TEM) and high-resolution scanning TEM (HR-STEM) image of the PbS : Na_2Se_2 = 4 : 1 shows high single crystallinity of nanoparticles and 3.01 Å distance of (200) lattice plane of PbS/PbSe. (Figure S3) A PbS and PbSe have a little different distance of (200) lattice plane of 2.97 Å and 3.06 Å, respectively. The (200) lattice plane distance of as-synthesized PbS/Se exists between the PbS and PbSe value. It could be one of the evidences of PbS/PbSe core/shell or alloy. The powder X-ray diffraction (XRD) patterns of the PbS and PbS/PbSe showed five prominent peaks, which were indexed to the (111), (200), (220), (222), and (420) planes of a cubic rock-salt structure at all compositions (Figure 1d). The linear shifts of peaks from PbS to PbSe by changing the molar ratio of PbS and Na_2Se_2 is an evidence of PbSe shell on the PbS nanoparticle surface, which can be explained by Vegard's law.¹⁷ To confirm the existence of selenium, inductively coupled plasma-atomic emission spectroscopy (ICP-AES) was performed. S element from PbS nanoparticle to Se precursor molar ratio of 4 : 1 resulted in nanocrystals with S to Se molar ratio of 6 : 1. Energy-dispersive X-ray spectroscopy scanning transmission electron microscopy (EDX-STEM) elemental analysis was performed to confirm the ICP-AES results. The Spectrum-2

areas in Supporting Information Figure S4, shows that the dots

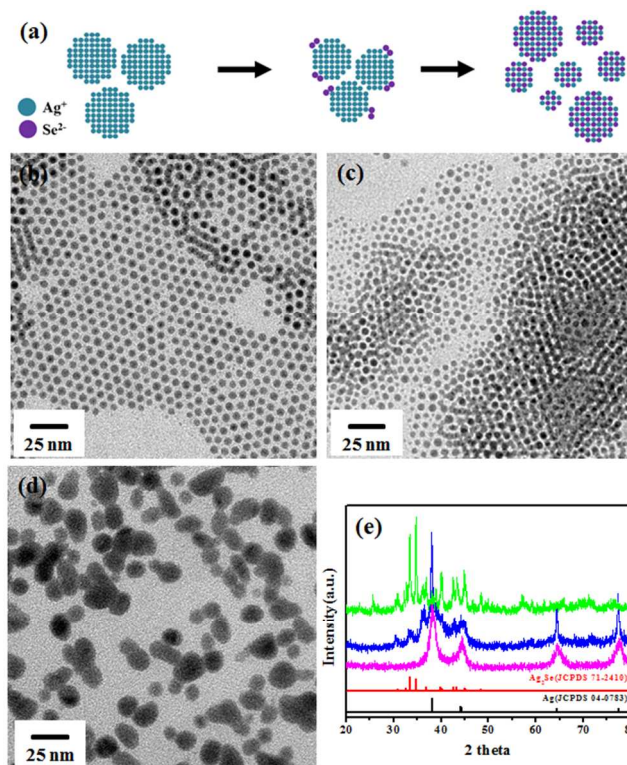


Figure 2. (a) Schematic illustration of synthetic mechanism from Ag to Ag_2Se nanoparticles. TEM image of (b) bare Ag, (c) Ag- Na_2Se_2 molar ratio 4 : 1, (d) Ag- Na_2Se_2 molar ratio 1 : 4. (e) X-ray diffraction patterns of bare Ag (pink), Ag- Na_2Se_2 molar ratio 4 : 1 (blue), Ag- Na_2Se_2 molar ratio 1 : 4 (green).

comprise Pb, S and Se elements. In order to investigate the elemental distribution in the PbS/PbSe nanoparticles, elemental mapping analysis of the nanoparticles was performed (Figure S5). While Se ion is relatively distributed outside of nanoparticle, S ion is distributed inside of nanoparticle. It's one of the evidence of PbS/PbSe core/shell. To compare the optical properties of them, UV-visible absorption measurements were performed. As adding the Na_2Se_2 molecules to the PbS nanoparticles in the room temperature, the band-edge absorption peak show a slightly blue-shift from 1264 nm to 1202 nm, which means that PbS core nanoparticle size became smaller. The small blue shift beyond our expectation result from the combination of size reduction and reverse type-I shell growth. The driving force of the anion exchange reaction can be assumed as follows; (i) high surface to volume ratio of nanocrystals provides an easy diffused pathway of atom, as a result, let high activation energy down (ii) PbS and PbSe have same cubic rock-salt structure, similar anionic radius of 170 pm and 184 pm, and similar lattice parameter of 0.593 nm and 0.612 nm, respectively (iii) PbS and PbSe have similar standard enthalpy of formation of -100.4 and -102.9 kJmol^{-1} at 298.15 K, respectively. Therefore, PbS and PbSe easily coexist homogeneous condition and S^{2-} anion can be exchanged with Se^{2-} at room temperature.

Figure 2a is schematic illustration of conversion of Ag nanoparticles to Ag_2Se nanoparticles, which involved sequential consumption of Ag and the growth of Ag_2Se . Figure 2b shows TEM image of 6.7 nm ($\sigma=0.3$) silver nanoparticles (Ag), which is synthesized by previously reported procedure. Silver selenide nanoparticles (Ag_2Se) were fabricated by adding Na_2Se_2 to an Ag

nanoparticle solution at room temperature. In order to investigate the

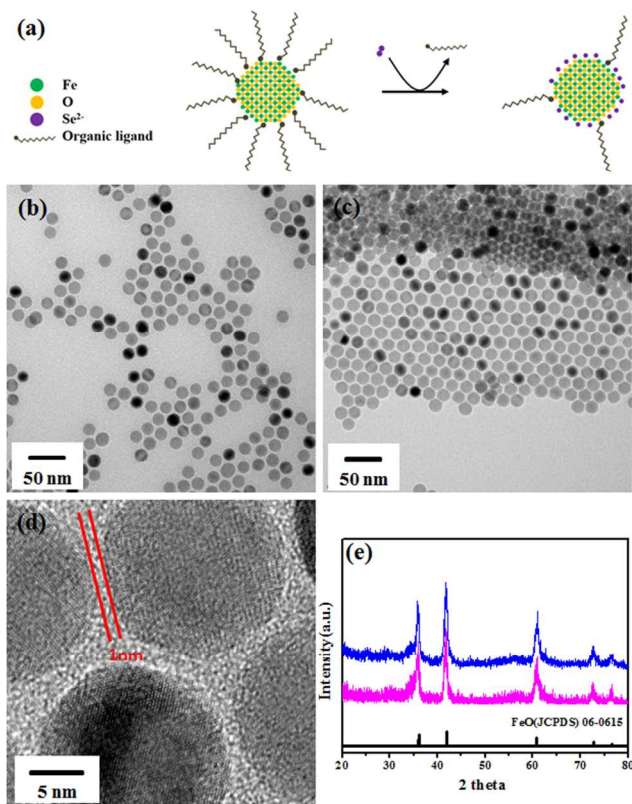


Figure 3. Schematic illustration of ligand exchange from oleic acid to Se^{2-} ion. TEM image of (b) bare FeO, (c) FeO- Na_2Se_2 . (d) high-resolution TEM images of Figure 3(c). (e) X-ray diffraction patterns of bare FeO (pink), FeO- Na_2Se_2 molar ratio 4 : 1 (blue)

elemental contents of the Ag and Ag_2Se nanoparticles mixture, ICP-AES analysis was performed. Ag nanoparticle to Se precursor molar ratio of 4 : 1 and 1 : 4 resulted in nanocrystals with Ag to Se molar ratio of 9 : 1 and 6 : 4, respectively. Figure 2c and Figure S6 are TEM images of Ag nanoparticle to Se precursor molar ratio of 4 : 1 and 8 : 1, which showed different sized nanocrystal of 6.1 nm and 5 nm, respectively. Compared with Ag nanoparticles (6.7 nm), their sizes are decreased as the Se adding. As the amount of Se ion increased, they dissolve the surface Ag atom of nanoparticles for Ag_2Se nanoparticle, thus Ag nanoparticle size is getting smaller and small sized Ag_2Se nanoparticles are formed. To prove our hypothesis more, we carried out the EDX-STEM analysis. The spectrum 6 and 7-labeled area in Supporting Information Figure S7, which point the area of 5 nm and less than 2 nm nanoparticle, respectively, shows that the former comprise Ag (that is Ag nanoparticles) and the latter Ag, Se elements (Ag_2Se nanoparticles). The results mean that large Ag nanoparticle are dissolved and small Ag_2Se nanoparticles are fabricated. To infer the mechanism around the selenium rich reaction (Figure 2d), as-synthesized small sized Ag_2Se nanoparticles agglomerate to form large sized Ag_2Se nanoparticles in one minute due to the self-focusing at the threshold point which is decided by selenium concentration.¹⁸ The HR-TEM image of the as-synthesized Ag_2Se shows high single crystallinity of nanoparticles and 2.68 Å distance of (112) lattice plane of Ag_2Se . (Figure S8) In order to investigate the elemental distribution in the Ag_2Se nanoparticles, elemental mapping analysis of the nanoparticles was performed (Figure S9). Ag and Se elements are equally distributed. The XRD

pattern of the Ag and Ag_2Se nanoparticles mixture (Figure 2e) shows that all diffraction patterns can be indexed to the peaks of Ag (JCPDS 04-0783) and Ag_2Se (JCPDS 71-2410) without impurities. The spontaneous transformation reaction of Ag to Ag_2Se nanoparticles can be postulated by the standard enthalpy of formation of Ag_2Se is -48.9 kJmol^{-1} at 298.15 K.

Figure 3a is schematic illustration of iron oxide reacting with Na_2Se_2 , which is acting as an inorganic ligand. FeO nanoparticles were synthesized using a Fe acetylacetonate and oleic acid as a precursor and a surfactant. This methodology is described in supporting information section. Figure 3b shows TEM images of 15 nm FeO nanoparticles, which have roughly 2~3 nm inter-particles distance because of steric repulsion of long chain organic ligand, especially oleic acid. When FeO nanoparticles mixed with Na_2Se_2 , they assemble to the superlattice structure and have about 1 nm inter-particles distance (Figure 3d), which means the replacement of oleic acid by selenium ion and as a result, the decrease of steric repulsion of long chain organic ligand on the surface. The reaction of FeO nanoparticles and Na_2Se_2 could not form the FeSe structure unlike the above Ag to Ag_2Se reaction because FeO is thermodynamically more stable than FeSe, which could be known by their standard enthalpy of formation. (FeO: -272 kJmol^{-1} , FeSe: -100 kJmol^{-1}) Therefore, Se^{2-} just remove the oleic acid on the FeO nanoparticles surface. To confirm the existence of selenium ion on surface, Zeta potential analysis was carried out. Bare FeO nanoparticles and FeO- Na_2Se_2 have a surface potential of -1.68 mV and -11.77 mV, respectively. The more minus potential value of FeO- Na_2Se_2 confirmed the existence of Se^{2-} on surface. There are no other change in particles size and XRD pattern. (Figure 3e). Thermogravimetric analysis (TGA) was performed to investigate the amounts of replaced oleic acid, which show about 40% and 20% volatile contents of FeO-Oleic acid (FeO capping with oleic acid) and FeO- Na_2Se_2 , respectively. (figure S10) The half of oleic acid is replaced with Se^{2-} , as a result, form the assembled superlattice structure.

In summary, we found a new applications area of alkali metal chalcogenides, very less research has been carried out on the synthesis and application unlike other chalcogenides until now. We synthesize alkali metal chalcogenides (disodium diselenide, Na_2Se_2) according to the literature with slight modification, which is acting as an anionic exchange reaction precursor (PbS to PbS/PbSe), Se precursor for metal selenide nanoparticles (Ag to Ag_2Se), and MCCs (FeO- Na_2Se_2) depending on the type of colloidal nanoparticles.

This work was supported by the New & Renewable Energy Core Technology Program of KETEP (No. 201330300001), Basic Science Research Program through the National Research Foundation of Korea (NRF) funded by the Ministry of Science, ICT & Future Planning (No. 2014R1A5A1009799) and the Priority Research Centers Program (2012-0006687), Republic of Korea.

Notes and references

^a Department of Molecular Science and Technology, Ajou University, Suwon, Gyeonggi-do 443-749, South Korea

^b Samsung Advanced Institute of Technology (SAIT), Samsung Electronics, 130 Samsung-ro Yeongtong, Suwon, Gyeonggi-do 446-712, South Korea

Correspondence equally

Sang-Wook Kim, Kyung-Sang Cho

Electronic Supplementary Information (ESI) available: [Supplementary figures, materials, experimental details, and synthetic methods.]. See DOI: 10.1039/c000000x/

- 1 N. Zheng, X. Bu and P. Feng, *Nature*, 2003, **426**, 428.
- 2 J. Lim, S. Jun, E. Jang, H. Baik, H. Kim and J. Cho, *Adv. Mater.*, 2007, **19**, 1927.
- 3 B. J. Eggleton, B. Luther-Davies and K. Richardson, *Nat. Photonics*, 2011, **5**, 141.
- 4 W. Liu, J.-S. Lee and D. V. Talapin, *J. Am. Chem. Soc.*, 2013, **135**, 1349.
- 5 C. B. Murray, D. J. Norris and M. G. Bawendi, *J. Am. Chem. Soc.*, 1993, **115**, 8706.
- 6 X. Peng, L. Manna, W. Yang, J. Wickham, E. Scher, A. Kadavanich and A. P. Alivisatos, *Nature*, 2000, **404**, 59.
- 7 E. Scalise, M. Houssa, G. Pourtois, V. Afanas'ev and A. Stesmans, *Nano Res.*, 2012, **5**, 43
- 8 A. Singh, A. Sanyal, C. O'Sullivan, F Laffir, C. Coughlan, K. M. Ryan and T. Bala, *Nano Res.*, 2013, **6**, 121
- 9 M. V. Kovalenko, M. Scheele and D. V. Talapin, *Science*, 2009, **324**, 1417.
- 10 J. Jang, W. Liu, J. S. Son and D. V. Talapin, *Nano Lett.*, 2014, **14**, 653.
- 11 M.-C. Daniel and D. Astruc, *Chem. Rev.*, 2004, **104**, 293.
- 12 A. R. Tao, S. Habas and P. Yang, *Small*, 2008, **4**, 310.
- 13 D. V. Talapin, J.-S. Lee, M. V. Kovalenko and E. V. Shevchenko, *Chem. Rev.*, 2010, **110**, 389.
- 14 J. Cusick and I. Dance, *Polyhedron*, 1991, **10**, 2629.
- 15 D. H. Son, S. M. Hughes, Y. Yin and A. P. Alivisatos, *Science*, 2004, **306**, 1009.
- 16 J. Park, H. Zheng, Y.-w. Jun and A. P. Alivisatos, *J. Am. Chem. Soc.*, 2009, **131**, 13943.
- 17 L. Vegard and H. Schjelderup, *Phys. Z.*, 1917, **18**, 93.
- 18 R. Xie and X. Peng, *Angew. Chem.*, 2008, **120**, 7791.